Chemistry & Biology
Article

DNA Replication Is the Target for the Antibacterial Effects of Nonsteroidal Anti-Inflammatory Drugs

Zhou Yin,[1] Yao Wang,[1] Louise R. Whittell,[1] Slobodan Jergic,[1] Michael Liu,[2] Elizabeth Harry,[2] Nicholas E. Dixon,[1] Michael J. Kelso,[1] Jennifer L. Beck,[1] and Aaron J. Oakley[1,*]
[1]School of Chemistry and Centre for Medical and Molecular Bioscience, University of Wollongong, Wollongong, NSW 2522, Australia
[2]iThree institute, University of Technology, Sydney, NSW 2007, Australia
*Correspondence: aarono@uow.edu.au
http://dx.doi.org/10.1016/j.chembiol.2014.02.009

SUMMARY

Evidence suggests that some nonsteroidal anti-inflammatory drugs (NSAIDs) possess antibacterial properties with an unknown mechanism. We describe the in vitro antibacterial properties of the NSAIDs carprofen, bromfenac, and vedaprofen, and show that these NSAIDs inhibit the *Escherichia coli* DNA polymerase III β subunit, an essential interaction hub that acts as a mobile tether on DNA for many essential partner proteins in DNA replication and repair. Crystal structures show that the three NSAIDs bind to the sliding clamp at a common binding site required for partner binding. Inhibition of interaction of the clamp loader and/or the replicative polymerase α subunit with the sliding clamp is demonstrated using an in vitro DNA replication assay. NSAIDs thus present promising lead scaffolds for novel antibacterial agents targeting the sliding clamp.

INTRODUCTION

Nonsteroidal anti-inflammatory drugs (NSAIDs) are widely used in the treatment of pain, fever, and inflammation (Vonkeman and van de Laar, 2010). Their mode of action is predominantly through inhibition of cyclooxygenases to reduce synthesis of the pro-inflammatory mediator prostaglandin H_2 (Dinarello, 2010). Other known targets of NSAIDs in inflammation include fatty acid amide hydrolase and phospholipase A2 (Singh et al., 2004, 2009; Bertolacci et al., 2013). Several off-targets unrelated to inflammation have been identified, including aldo-ketoreductase 1C3 and retinoid X receptor-α. Binding to these proteins may explain some of the antiproliferative effects of NSAIDs (Zhou et al., 2010; Flanagan et al., 2012). Limited data suggest that NSAIDs possess antibacterial properties, although these are confounded by routine use of NSAIDs in combination with antibiotics (Origlieri and Bielory, 2009), particularly in veterinary medicine (Elitok and Elitok, 2004; Lopez et al., 2007; Krömker et al., 2011). Weak in vitro antibacterial activity has been demonstrated by ibuprofen and indomethacin (Shirin et al., 2006; Al-Janabi, 2010), but there has been no report of a mechanism for this action.

Our studies on the *Escherichia coli* DNA polymerase III (Pol III) β subunit led to the discovery that the NSAID carprofen binds to and inhibits essential interactions of this protein. Pol III β, also known as the sliding clamp (SC) is a torus-shaped homodimer that is structurally conserved among all bacterial species (Burnouf et al., 2004; Argiriadi et al., 2006; Gui et al., 2011) and serves as a protein-protein interaction hub during DNA replication and repair (Dalrymple et al., 2001; Johnson and O'Donnell, 2005; Indiani and O'Donnell, 2006). After being loaded onto double-stranded DNA through interactions with the δ subunit of the Pol III clamp loader complex (composed of Pol III $\delta(\gamma/\tau)_3\delta'$; Naktinis et al., 1995; Jeruzalmi et al., 2001; Leu and O'Donnell, 2001), the SC recruits a diverse range of protein binding partners, including the α and ε subunits of Pol III; DNA polymerases I, II, IV, and V; and MutS (Kong et al., 1992; Indiani and O'Donnell, 2006; Jergic et al., 2013). This array of binding partners makes the SC one of the most trafficked elements in the cell (Bunting et al., 2003; López de Saro, 2009; Robinson et al., 2012). It confers high processivity upon the Pol III αεθ core (the replicase) by acting as a mobile tether (Beck et al., 2006; Kelch et al., 2011).

A single binding pocket containing two subsites (I and II; Burnouf et al., 2004; Georgescu et al., 2008) located on each of the SC monomers interacts with short linear clamp-binding motifs (CBMs) located in flexible C-terminal regions or internal loops of known protein binding partners (Kong et al., 1992; Shamoo and Steitz, 1999; Dalrymple et al., 2001). Studies have identified a consensus CBM sequence QLx_1Lx_2F/L (where x is any amino acid; S or D preferred at x_1; x_2 may be absent) that interacts with the SC CBM-binding pocket, and isolated peptides based on this sequence bind the SC with affinities similar to their parent proteins (Wijffels et al., 2004, 2011). Conversely, when CBMs are removed from parent proteins, they are observed to lose affinity for the SC (Dalrymple et al., 2001; Kongsuwan et al., 2006).

Targeting the bacterial DNA replication machinery is a validated strategy for producing clinically useful antibiotics, as evidenced by the highly successful quinolones, DNA gyrase inhibitors (Kohanski et al., 2010). The bacterial SC is an emerging DNA replication target that is yet to be clinically validated (Robinson et al., 2012). Modified peptides based on the consensus sequence show increased affinity to the clamp (Wolff et al., 2011; Wijffels et al., 2011). Small molecules have been identified

Table 1. *E. coli* SC Binding Properties and Antibacterial Activities of Selected NSAIDs

	E. coli SC Inhibition		MIC[a]							
			E. coli		*A. baylyi*		*S. aureus*		*B. subtilis*	
NSAID	IC_{50} (μM)	K_i[b] (μM)	μM	μg/ml	μM	μg/ml	μM	μg/ml	μM	μg/ml
Vedaprofen	222	131	5,000	1,410	2,500	705	156	44	156	44
Bromfenac	328	193	2,500	835	5,000	1,670	2,500	835	1,250	418
Carprofen	481	283	2,500	680	1,250	340	313	85	313	85
Flufenamic acid	~1,300	~750	>5,000	>1,400	5,000	1,400	625	175	313	88
Tolfenamic acid	~1,500	~900	>5,000	>1,300	5,000	1,300	625	163	313	82

See also Tables S1–S3 and Figure S1.

[a]MIC was determined as the lowest NSAID concentration giving a background-corrected OD_{595} < 0.1 after 24 hr of bacterial growth.

[b]K_i is calculated from IC_{50} values using the Kenakin correction for ligand depletion (Kenakin, 1993).

that bind to the CBM-binding pocket of the SC and inhibit interactions with polymerases, but no antibacterial activities have yet been reported (Georgescu et al., 2008; Wijffels et al., 2011). These are RU7, a thioxothiazolinine derivative (Georgescu et al., 2008), and a biphenyloxime ether derivative (Wijffels et al., 2011). Both classes of compound bind in subsite I of the CBM-binding cleft. Our observation of the ability of the NSAID carprofen, described below, to bind to the identical site on the SC spurred us to initiate a broader exploration of the effects of NSAIDs on the SC. Minimal inhibitory concentrations (MICs) were measured for a variety of NSAIDs to establish a correlation between SC binding and inhibition and in vitro antibacterial potencies. Biochemical assays using a minimal set of components for SC-dependent DNA replication were used to demonstrate inhibitory effects of NSAIDs on this essential process, and X-ray crystallography provided structural insights into NSAID-SC binding.

RESULTS

SC Inhibition and Antibacterial Potency

A fluorescence polarization (FP) competition assay (Yin et al., 2013) was used to assess the *E. coli* SC binding affinity of commercially available NSAIDs. A fluorescently labeled tracer peptide (5-carboxyfluorescein-QLDLF) based on the *N*-acetylated consensus pentapeptide AcQLDLF (Wijffels et al., 2011; Wolff et al., 2011) was used as the competitor ligand. Inhibition of tracer binding to the SC at various NSAID concentrations gave half-maximal inhibitory concentration (IC_{50}) values that were transformed into inhibition constants (K_i) using the Kenakin correction for ligand depletion (Kenakin, 1993). Twenty NSAIDs were tested (Table S1 available online), with five showing K_i values in the high micromolar range (Table 1; Figure S1). Vedaprofen, bromfenac, and carprofen showed the strongest effects (K_i < 300 μM), while flufenamic and tolfenamic acids were weaker binders (K_i values > 700 μM).

NSAIDs were tested for antibacterial activity using standard MIC assays with four species: *E. coli*, *Acinetobacter baylyi*, *Staphylococcus aureus*, and *Bacillus subtilis*. MICs evaluated as inhibited visible growth with varying concentrations of NSAIDs are provided in Table S1. The Gram-positive species (*S. aureus* and *B. subtilis*) showed higher susceptibility to NSAIDs than the Gram-negative species (*E. coli* and *A. baylyi*), a trend also observed with four positive control antibiotics (Table S2). The additional permeability barrier of the outer membrane in Gram-negative species is likely responsible for these trends (Rigel and Silhavy, 2012).

The antibacterial testing was repeated for the top-five SC inhibitors, vedaprofen, bromfenac, carprofen, and flufenamic and tolfenamic acids. The MICs were determined as lowest NSAID concentration with background-corrected optical density of less than 0.1 after 24 hr bacterial growth (Table S3). The resulting MICs (Table 1; data derived from Table S3) are consistent with results from visual inspections. These five NSAIDs that most potently inhibited *E. coli* SC binding in the FP assay were the same compounds that showed the highest level of antibacterial activity against Gram-positive species and were the only NSAIDs to show any activity against the Gram-negative species. NSAIDs that did not inhibit the *E. coli* SC all showed very low or negligible antibacterial activity (Table S1), consistent with inhibition of the SC giving rise to the antibacterial effects of NSAIDs. The consensus pentapeptide AcQLDLF (Wolff et al., 2011) showed high affinity for the *E. coli* SC (K_i ~1 μM), but no antibacterial activity (Table S1), likely due to its inability to penetrate bacterial membranes (Bechara and Sagan, 2013) and/or susceptibility to aminopeptidase activity (Gonzales and Robert-Baudouy, 1996).

NSAIDs Inhibit the *E. coli* SC through Binding to Subsite I of the CBM-Binding Pocket

The locations of binding of NSAIDs to the *E. coli* SC were demonstrated by X-ray crystallography. NSAID/*E. coli* SC co-crystal structures were obtained with each of the best SC binders, vedaprofen, bromfenac, and carprofen. These complexes are denoted as $SC^{Vedaprofen}$, $SC^{Bromfenac}$, and $SC^{Carprofen}$. All three NSAIDs were found to bind in subsite I of the CBM-binding pocket (Figure 1). Interestingly, while crystals were soaked in the presence of racemic mixtures of vedaprofen and carprofen, the *2mFo-DFc* electron density maps suggested that (*R*)-vedaprofen and (*S*)-carprofen were the favored stereoisomers in the complexes (Figures 1A and 1C). Superimpositions of the NSAID-bound structures and their corresponding native crystal structures (obtained in the same crystal form) are shown in Figures 1A–1C. Stereo diagrams of these complex structures are shown in Figure S1.

The cyclohexyl moiety of (*R*)-vedaprofen occupies a deep hydrophobic pocket in subsite I comprising the side chains of V247, L177, V360, and M362 (Figure 1A). The naphthalene rings

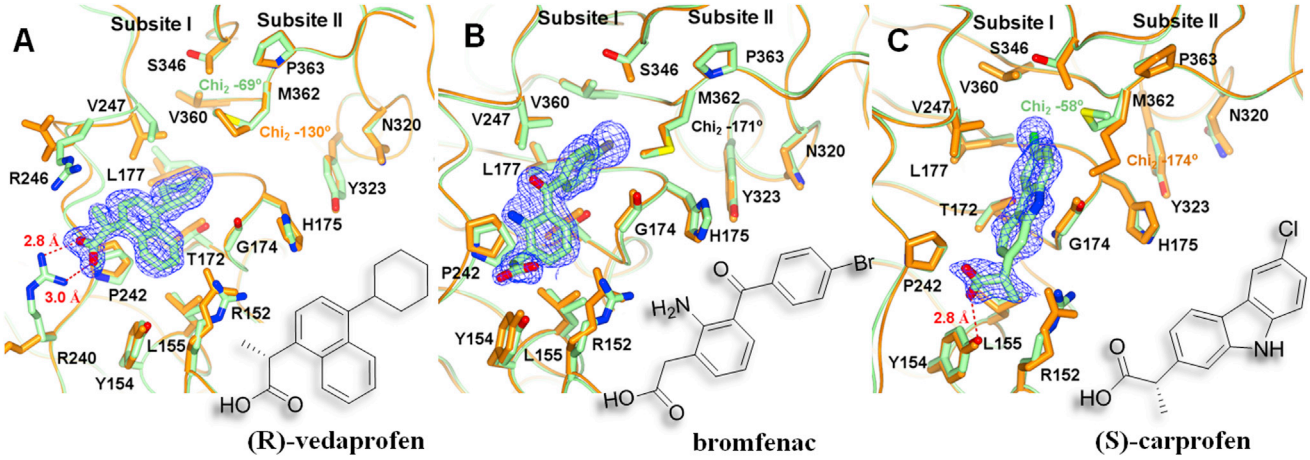

Figure 1. X-Ray Crystal Structures Showing NSAIDs Bound to Subsite I of the CBM-Binding Pocket of the *E. coli* Sliding Clamp

Complexes are represented with the SC and NSAID carbon atoms in shaded light green. (*R*)-vedaprofen (A), bromfenac (B), and (*S*)-carprofen (C). All other atoms are represented in CPK colors. Apo-SC structures (Yin et al., 2013; PDB entries 4K3P chain B in A and 4K3S chain A in B and C, shown in orange) are superimposed for comparison. Pairs of H-bonded atoms are indicated with dashed red lines. Electron density maps ($2mF_o$–DF_c) contoured at 1σ are shown in blue wire-basket form.

See Figure S1 for stereo views and Table S4 for crystallographic details.

occupy an adjacent, shallower region near P242. Binding of (*R*)-vedaprofen moved the side chains of R246 and R240 (relative to the apo-SC structure) toward the (*R*)-vedaprofen carboxylate, resulting in formation of a salt bridge between the carboxylate and the guanidinium moiety of R240. The side chain of V247 adopted a flipped conformation relative to the apo structure, apparently as a result of steric interactions with the bulky cyclohexane group. Additionally, the cyclohexyl ring caused rotation of the χ_2 angle of M362, a residue that acts as a "gate" between subsites I and II, from −130° to −69°. The side chain of S346 was also rotated in response to movements in M362.

The aryl bromide of bromfenac occupies the deep hydrophobic pocket of subsite I, with the aniline group residing in the adjacent shallower region (Figure 1B). The carboxylate of bromfenac makes no direct interactions with the binding site. Binding of bromfenac caused only minor structural perturbations in subsite I with the exception of a rotated side chain at S346. The "gating" residue M362 retained the "closed" conformation (χ_2 of −171°), as observed in the apo-SC structure.

In the case of (*S*)-carprofen, the carbazole ring occupies the shallower region and the aryl chloride is buried in the adjacent deep pocket (Figure 1C). The carboxylate group of (*S*)-carprofen forms an H-bond with the side chain phenol of Y154. The carbazole nitrogen is oriented outward from the binding site and this pose appears to open the M362 gate, rotating its χ_2 angle from −174° to −58°. The only other change observed in subsite I is the rotation of the side chain of S346.

The *E. coli* SC CBM-Binding Pocket Is Conserved across Bacterial Species

Sequence alignments of the SCs (Figure 2A) from the four bacterial species used in the antibacterial assays show that the 15 residues comprising subsites I (yellow) and II (cyan) of their respective CBM-binding pockets are very well conserved, especially in subsite I. Sequence alignments of the SCs from a total of nine bacterial species (five Gram-negative species and four Gram-positive species) similarly showed highly conserved CBM-binding pocket sequences (Figure S2).

The structures of $SC^{Carprofen}$ and the *E. coli* SC in complex with the Pol III δ subunit (Protein Data Bank [PDB] entry 1JQJ; Jeruzalmi et al., 2001) are overlaid in Figure 2B. Similarly, the structures of $SC^{Carprofen}$ and the SC in complex with the C-terminal CBM-peptide of the Pol III α subunit (PDB entry 3D1F; Georgescu et al., 2008) are overlaid in Figure 2C. The structures show that binding of the CBMs of both Pol III δ and α subunits span subsites I and II, with the LxF submotif of each peptide filling the pocket at subsite I occupied by the NSAIDs (Figures 1A and 1B). High sequence conservation within the CBM-binding pockets of the various SC homologs suggests that these NSAIDs most likely bind to subsite I and inhibit the SCs of many bacterial species.

NSAIDs Inhibit In Vitro DNA Replication

An SC-dependent DNA replication assay using a minimal set of components required for in vitro DNA replication was developed to explore inhibition of the *E. coli* SC by NSAIDs. In this assay, binding of CBMs from the δ and α subunits to the SC are essential for replication, meaning impaired SC binding due to the presence of NSAIDs will inhibit DNA synthesis. A synthetically RNA-primed circular single-stranded (ss) DNA coated with ss DNA-binding protein (SSB) was used as a template. The reaction system (Jergic et al., 2013) contained the SC, the Pol III α subunit, and a reconstituted clamp loader complex ($\gamma_3\delta\delta'$) to load the SC at the primer terminus (Figure 3A). The α subunit bound to the SC catalyzes extension of the primer through incorporation of deoxyribonucleoside triphosphates (dNTPs) using the ssDNA as template. Formation of double-stranded DNA was tracked by agarose gel electrophoresis and is dependent on the SC concentration (Figures S3A and S3B).

As a positive control, the pentapeptide AcQLDLF (K_i ~1 μM; used as a model inhibitor) showed dose-dependent inhibition of replication over the range of 1–10 μM (Figure 3B), when added

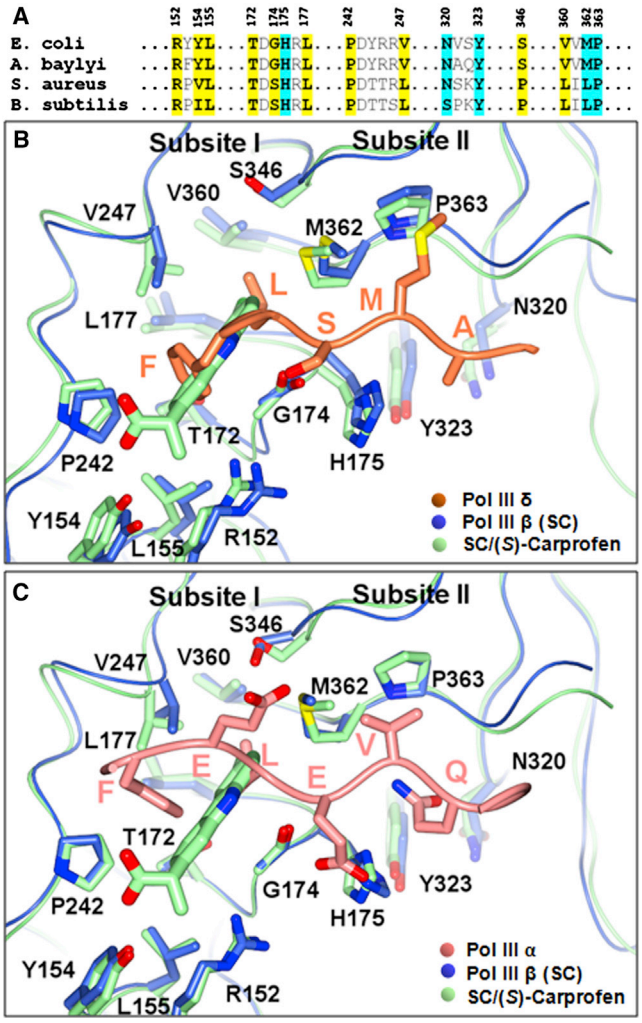

Figure 2. NSAIDs at the CBM Binding Site of the *E. coli* SC

(A) Sequence alignments of SCs from the four bacterial species. Residues comprising subsites I (yellow) and II (cyan) of the CBM-binding pockets (numbering based on the *E. coli* sequence) are highlighted. See also Figure S2.

(B and C) Superimposition of the structures of the *E. coli* SC in complex with (B) (*S*)-carprofen and the CBM of Pol III δ (PDB entry 1JQJ; Jeruzalmi et al., 2001) and (C) (*S*)-carprofen and the C-terminal CBM peptide of Pol III α (PDB entry 3D1F; Georgescu et al., 2008). The SC and (*S*)-carprofen carbon atoms are in shaded light green. The SC carbon atoms in PDB entries 1JQJ and 3D1F are in blue with the carbon atoms of the Pol III δ and α subunits in orange and pink, respectively. All other atoms are represented in CPK colors. Only the residues of the δ and α subunits that interact with subsites I and II are shown for clarity.

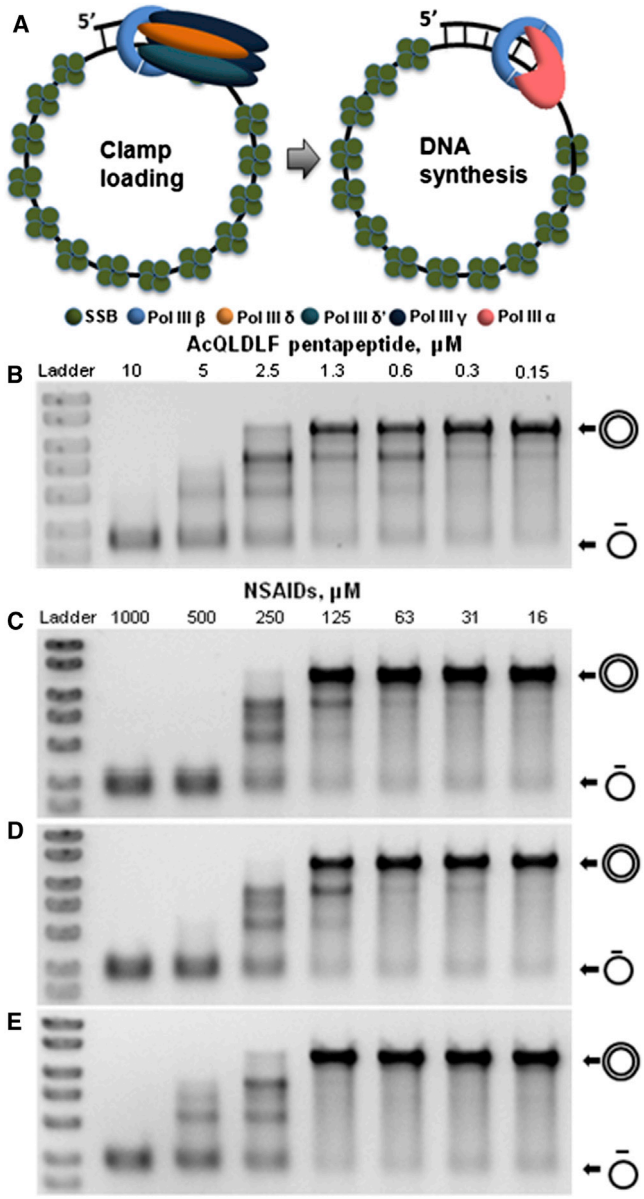

Figure 3. NSAIDs Inhibit In Vitro DNA Replication

(A) Components of the replication assay.

(B–E) Inhibition of DNA synthesis by AcQLDLF (B), and NSAIDs vedaprofen (C), bromfenac (D), and carprofen (E). The ssDNA template is converted to a double-stranded circular product, as indicated.

See also Figure S3.

to the complete replication system. A titration was also carried out by pre-incubating the reaction system before the addition of the α subunit and the AcQLDLF pentapeptide, hoping to distinguish the inhibition of DNA synthesis from the inhibition of clamp loading (Figure S3C). However, two experiments yielded similar inhibition profiles, suggesting that ongoing synthesis by α from a preloaded SC is at least as sensitive to inhibition as clamp loading. The reversible nature of clamp-loading (Leu et al., 2000) also provides a plausible explanation for the similar profiles—the addition of an inhibitor followed by equilibration of the clamp-loading and unloading process erases the effects of pre-incubation.

NSAIDs were titrated into the total reaction system at concentrations up to 1 mM (Figures 3C–3E). Vedaprofen and bromfenac completely inhibited replication at 500 μM, while showing no effects below 63 μM. Carprofen showed weaker effects consistent with its weaker affinity for the SC (Table 1), producing complete inhibition at 1 mM. Inhibitory potencies of NSAIDs in the DNA replication assay were approximately 100-fold less than those for AcQLDLF, consistent with their ~100-fold weaker

SC-binding affinities. Assays carried out with the less potent SC binders flufenamic and tolfenamic acids and the non-SC binding NSAID ibuprofen showed much weaker effects or no inhibition of DNA replication (Figures S3D and S3E).

DISCUSSION

There is a pressing need for new classes of antibiotics (Bassetti et al., 2013). The bacterial SC is an emerging target for the development of new antibacterial agents (Georgescu et al., 2008; Wijffels et al., 2011). Its structure is highly conserved: studies indicate that clamps from several bacterial species have similar overall structures and CBM-binding sites (Burnouf et al., 2004; Argiriadi et al., 2006; Gui et al., 2011). This study demonstrates that some NSAIDs are able to block subsite I, preventing SC binding to Pol III δ and/or α subunits and causing inhibition of DNA replication in vitro. Bacterial DNA replication in vivo is highly complex and involves many interacting components (Kelman and O'Donnell, 1995; Pomerantz and O'Donnell, 2007). By simplifying replication to a requirement for just four essential components, the SC, the clamp loader complex, the Pol III α subunit, and SSB (Jergic et al., 2013), we were able to directly link inhibition of SC-mediated interactions by NSAIDs to inhibition of DNA replication in vitro, thus providing an explanation for the apparent correlation between *E. coli* SC inhibition and antibacterial effects. Because the CBM-binding pocket is well conserved across bacteria, *E. coli* SC inhibitors like vedaprofen, bromfenac, and carprofen would also be expected to bind SCs from other species. All three were shown to be relatively weak inhibitors of the *E. coli* SC, consistent with their modest antibacterial activity compared to standard antibiotics. It is noteworthy that bromfenac demonstrated much weaker antibacterial activity against Gram-positive species than vedaprofen and carprofen. Furthermore, flufenamic and tolfenamic acids exhibited similar antibacterial effects to carprofen despite apparent weak SC affinity. These observations could be explained in part by differing membrane permeability and differences in the SC affinities of those compounds in the different species. While vedaprofen and carprofen have been used as adjuvants to antibiotics for their anti-inflammatory effects in the treatment of veterinary bacterial infections (Elitok and Elitok, 2004; Lopez et al., 2007; Krömker et al., 2011), the current work suggests that their co-administration may actually contribute independent (or perhaps synergistic) antibacterial effects.

The X-ray structures here, showing that the three NSAIDs bind in subsite I, should provide valuable insights into the design of more potent small-molecule SC inhibitors, potentially leading to the discovery of new classes of antibiotics with a novel mechanism of action. The conserved nature of the SC across bacterial species suggests potent SC inhibitors might show broad-spectrum activity. All three NSAIDs were shown to bury a hydrophobic moiety into the deep pocket of subsite I while positioning an aromatic ring(s) in the adjacent and shallower region. The three NSAIDs all contained carboxylic acids, which can form salt-bridges or H-bonds with adjacent residues; however, these interactions appeared to be confined to the edge of subsite I and did not seem to be a prerequisite for binding. Whereas all three NSAIDs fully occupied subsite I, their relatively weak binding suggests there is only limited potential for designing more potent SC inhibitors that target subsite I alone. Of the three NSAIDs, only carprofen adopted a binding pose that "opened" the M362 gate separating the two subsites, inducing a CBM-binding pocket structure similar to that observed upon binding of peptide CBMs. It was also noted that the carbazole nitrogen of carprofen is directed toward subsite II, suggesting it might be a useful synthetic handle for projecting extra functionality toward this subsite in searching for nonpeptidic SC-binders with higher affinity.

SIGNIFICANCE

New classes of antibiotics operating through novel targets are of great interest. The sliding clamp represents an emerging target for new antibacterial agents—interactions between DNA polymerases and sliding clamps are essential to ensure DNA replication and cell proliferation. Sliding clamp inhibitors have been reported, but none are yet used therapeutically. We report antibacterial activity of members of an established drug class, the nonsteroidal anti-inflammatory drugs (NSAIDs) against Gram-negative and Gram-positive bacteria, and link those activities to inhibition of sliding clamps.

EXPERIMENTAL PROCEDURES

Compounds and Peptides

NSAIDs (purity > 95%) were purchased from Vitas-M Laboratory, Labotest, or Sigma-Aldrich. Peptides were custom synthesized by GL Biochem (China) and showed >95% purity, as confirmed by high-performance liquid chromatography-mass spectrometry.

Protein Expression and Purification

Expression and purification of the *E. coli* SC, Pol III α subunit, SSB, and the clamp loader complex $\gamma_3\delta\delta'$ were carried out as described previously (Wijffels et al., 2004; Mason et al., 2013; Jergic et al., 2013).

Crystallization and X-Ray Data Collection

Crystals of the *E. coli* SC were grown at 285 K by the hanging-drop vapor diffusion method. The drop was composed of 1 μl of sliding clamp (53 mg/ml in 10 mM Tris-HCl pH 7.2, 1 mM dithiothreitol, 1 mM EDTA, and 15% glycerol) mixed with an equal volume of reservoir solution consisting of 100 mM 2-(N-morpholino) ethanesulfonic acid buffer pH 6.5, 100–150 mM $CaCl_2$, and 25%–30% (v/v) PEG400.The reservoir volume was 1 ml. SC crystals were transferred to a $CaCl_2$-free reservoir solution and ligands were soaked into the crystal at 2–5 mM in reservoir solution with <10% DMSO. All crystals were mounted using MiTeGen loops on pins with magnetic caps. For in-house data collection, crystals were flash-frozen to 100 K using an Oxford Cryo-stream. Diffraction data were collected using a MAR345 desktop beamline using CuKα X-rays from a Rigaku 007HF rotating anode generator with Varimax optics. For synchrotron data collection, the SSRL automated mounting system (SAM) was used. Mounted crystals were flash-frozen in liquid nitrogen and placed in the SAM cassettes. Diffraction data were collected at 100 K at the Australian Synchrotron, Beamline MX1 using X-rays of wavelength 0.95 Å.

Data Processing, Structure Solution, and Refinement

Crystal data sets were integrated, merged, and scaled with either HKL2000 (Otwinowski and Minor, 1997) or MOSFLM and SCALA (Winn et al., 2011) The structures were solved by molecular replacement with CCP4 using the PDB entry 1MMI (Oakley et al., 2003) or 4K3S (Yin et al., 2013) as the starting model. Iterative cycles of model building and refinement were performed in COOT (Emsley and Cowtan, 2004) and REFMAC5 (Skubák et al., 2004).

Bioinformatics

Sequence alignment of bacterial sliding clamps (Gene Expression Onmibus IDs: YP_859300.1, WP_004930066.1, ZP_05582848.1, ZP_08441263.1, NP_064722.1, NP_373240.1, WP_003242509.1, YP_815419.1, and AAF98349.2) was carried out using COBALT (Papadopoulos and Agarwala, 2007).

Fluorescence Polarization Assay

FP experiments followed the published protocol (Yin et al., 2013). Brifely, All FP experiments were conducted using a POLARstar Omega plate reader with nontreated black sterile 96-well plates (Greiner). The buffer contained 10 mM HEPES pH 7.4, 1 mM EDTA, 1 mM dithiothreitol, 0.07% Nonidet P-40, and 5% DMSO. The fluorescent tracer used was *N*-fluorescein (FAM)-QLDLF-OH (GL Biochem), which has a K_d of 70 nM for SC monomers. For the competition assay, 10 nM peptide and 50 nM sliding clamp monomers were used. Blank control (buffer), negative control (buffer and the peptide), and positive control (buffer, peptide, and the sliding clamp) were used for data standardization. Experiments were carried out in duplicate. Curves were fit using GraphPad Prism v5.01 (GraphPad Software). Binding-saturation curve fitting was applied to tracer binding. Dose-response curve fitting was applied to competition assays with variable slope.

Antibacterial Activity

Determination of MICs was carried out with the four bacterial strains *Acinetobacter baylyi* ADP1, *Escherichia coli* K12 MG1655, *Staphylococcus aureus* NCTC8325, and *Bacillus subtilis* 168. Experiments followed the Clinical and Laboratory Standards Institute broth microdilution method (CLSI, 2009). Briefly, bacteria were grown overnight and inoculated at 5×10^4 colony-forming units/ml into cation-adjusted Mueller Hinton II broth. Serial 2-fold dilution of NSAID compounds or antibiotics was carried out in sterile 96-well plates. Controls of the growth medium only (blank controls), inoculated medium (negative controls), and inoculated medium with antibiotics (as positive controls) were used. Tests were carried out with 20 NSAIDs and four antibiotics, where MICs were defined as the lowest concentration of compound to inhibit visible growth after incubation for 24 hr at 37°C. For vedaprofen, bromfenac, carprofen, and flufenamic and tolfenamic acids, optical density values of inoculated cultures were measured at wavelength 595 nm (OD_{595}) as the background using a plate reader (Tecan Infinite M200 Pro). The plates were incubated for 24 hr at 37°C and then the OD_{595} values were measured again; MICs were defined as the lowest compound concentration with background-subtracted $OD_{595} < 0.1$.

DNA Replication Assay

The RNA-primed DNA template was prepared in advance by mixing 35 nM wild-type M13 ssDNA (Jergic et al., 2013) with 1 μM oligoribonucleotide (5′-UAUGUACCCCGGUUGAUAAUCAGAAAAGCCCCA; GeneWorks) in 30 mM Tris-HCl pH 7.6, 15 mM $MgCl_2$, 130 mM NaCl, and 0.1 mM EDTA for 10 min at 55°C and cooling to room temperature over 8 hr. DNA replication assays contained 20 mM Tris-HCl pH 7.6, 10 mM $MgCl_2$, 0.8 mM ATP, 8.4 mM dithiothreitol, 0.6 mM of each dNTP, 211 nM Pol III α subunit, 700 nM SSB (as tetramers), 210 nM Pol III β subunit (as dimers), 42 nM $\gamma_3\delta\delta'$ clamp loader complex, 120 mM NaCl, and 3 nM RNA primed DNA template, in a volume of 6.8 μl. Compounds/peptide were dissolved in DMSO and diluted in series 2-fold (in 50% v/v DMSO) before being added (0.5 μl) to the assay mixture at 0°C. The final DMSO concentration was 3.4% (v/v) in all assays. The assay mixtures were treated at 30°C for 60 min before being quenched by the addition of EDTA to 150 mM and SDS to 1% (w/v). The DNA products were separated by 0.7% agarose gel electrophoresis in TAE buffer (80 mM Tris, 40 mM acetic acid, and 4 mM EDTA) and then stained with 10,000-fold diluted SYBR Gold (Life Technologies) for 60 min. The DNA products were visualized using a UV transilluminator.

ACCESSION NUMBERS

The PDB accession codes for the atomic coordinates and structure factors for $SC^{Vedaprofen}$, $SC^{Bromfenac}$, and $SC^{Carprofen}$ are 4MJP, 4MJQ, and 4MJR, respectively.

SUPPLEMENTAL INFORMATION

Supplemental Information includes three figures and four tables and can be found with this article online at http://dx.doi.org/10.1016/j.chembiol.2014.02.009.

AUTHOR CONTRIBUTIONS

A.J.O., N.E.D., E.J.H., L.R.W., M.J.K., and J.L.B. supervised the project; Z.Y., Y.W., and A.J.O. designed the experiments; Z.Y. performed the fluorescence polarization-based assays, X-ray crystallography experiments, and antibacterial testing with assistance by M.L.; Y.W. and S.J. prepared proteins and performed replication assays; and Z.Y. and Y.W. drafted the manuscript with input from all co-authors.

ACKNOWLEDGMENTS

We thank the staff at Beamline MX1, Australian Synchrotron. This research was supported by an Australian Research Council (ARC) Discovery Project (DP110100660) and National Health and Medical Research Council (Australia) Project Grant (1021479). A.J.O. acknowledges support from the ARC for his Future Fellowship (FT0990287).

Received: December 11, 2013
Revised: February 3, 2014
Accepted: February 13, 2014
Published: March 13, 2014

REFERENCES

Al-Janabi, A.A.H.S. (2010). *In vitro* antibacterial activity of ibuprofen and acetaminophen. J Glob Infect Dis *2*, 105–108.

Argiriadi, M.A., Goedken, E.R., Bruck, I., O'Donnell, M., and Kuriyan, J. (2006). Crystal structure of a DNA polymerase sliding clamp from a gram-positive bacterium. BMC Struct. Biol. *6*, 2.

Bassetti, M., Merelli, M., Temperoni, C., and Astilean, A. (2013). New antibiotics for bad bugs: where are we? Ann. Clin. Microbiol. Antimicrob. *12*, 22.

Bechara, C., and Sagan, S. (2013). Cell-penetrating peptides: 20 years later, where do we stand? FEBS Lett. *587*, 1693–1702.

Beck, J.L., Urathamakul, T., Watt, S.J., Sheil, M.M., Schaeffer, P.M., and Dixon, N.E. (2006). Proteomic dissection of DNA polymerization. Expert Rev. Proteomics *3*, 197–211.

Bertolacci, L., Romeo, E., Veronesi, M., Magotti, P., Albani, C., Dionisi, M., Lambruschini, C., Scarpelli, R., Cavalli, A., De Vivo, M., et al. (2013). A binding site for nonsteroidal anti-inflammatory drugs in fatty acid amide hydrolase. J. Am. Chem. Soc. *135*, 22–25.

Bunting, K.A., Roe, S.M., and Pearl, L.H. (2003). Structural basis for recruitment of translesion DNA polymerase Pol IV/DinB to the β-clamp. EMBO J. *22*, 5883–5892.

Burnouf, D.Y., Olieric, V., Wagner, J., Fujii, S., Reinbolt, J., Fuchs, R.P.P., and Dumas, P. (2004). Structural and biochemical analysis of sliding clamp/ligand interactions suggest a competition between replicative and translesion DNA polymerases. J. Mol. Biol. *335*, 1187–1197.

CLSI (2009). Methods for dilution antimicrobial susceptibility tests for bacteria that grow aerobically; approved standard. (Wayne, PA: CLSI).

Dalrymple, B.P., Kongsuwan, K., Wijffels, G., Dixon, N.E., and Jennings, P.A. (2001). A universal protein-protein interaction motif in the eubacterial DNA replication and repair systems. Proc. Natl. Acad. Sci. USA *98*, 11627–11632.

Dinarello, C.A. (2010). Anti-inflammatory agents: Present and future. Cell *140*, 935–950.

Elitok, B., and Elitok, O.M. (2004). Clinical efficacy of carprofen as an adjunct to the antibacterial treatment of bovine respiratory disease. J. Vet. Pharmacol. Ther. *27*, 317–320.

Emsley, P., and Cowtan, K. (2004). Coot: model-building tools for molecular graphics. Acta Crystallogr. D Biol. Crystallogr. *60*, 2126–2132.

Flanagan, J.U., Yosaatmadja, Y., Teague, R.M., Chai, M.Z., Turnbull, A.P., and Squire, C.J. (2012). Crystal structures of three classes of non-steroidal anti-inflammatory drugs in complex with aldo-keto reductase 1C3. PLoS ONE *7*, e43965.

Georgescu, R.E., Yurieva, O., Kim, S.S., Kuriyan, J., Kong, X.P., and O'Donnell, M. (2008). Structure of a small-molecule inhibitor of a DNA polymerase sliding clamp. Proc. Natl. Acad. Sci. USA *105*, 11116–11121.

Gonzales, T., and Robert-Baudouy, J. (1996). Bacterial aminopeptidases: properties and functions. FEMS Microbiol. Rev. *18*, 319–344.

Gui, W.J., Lin, S.Q., Chen, Y.Y., Zhang, X.E., Bi, L.J., and Jiang, T. (2011). Crystal structure of DNA polymerase III β sliding clamp from *Mycobacterium tuberculosis*. Biochem. Biophys. Res. Commun. *405*, 272–277.

Indiani, C., and O'Donnell, M. (2006). The replication clamp-loading machine at work in the three domains of life. Nat. Rev. Mol. Cell Biol. *7*, 751–761.

Jergic, S., Horan, N.P., Elshenawy, M.M., Mason, C.E., Urathamakul, T., Ozawa, K., Robinson, A., Goudsmits, J.M., Wang, Y., Pan, X., et al. (2013). A direct proofreader-clamp interaction stabilizes the Pol III replicase in the polymerization mode. EMBO J. *32*, 1322–1333.

Jeruzalmi, D., Yurieva, O., Zhao, Y., Young, M., Stewart, J., Hingorani, M., O'Donnell, M., and Kuriyan, J. (2001). Mechanism of processivity clamp opening by the δ subunit wrench of the clamp loader complex of *E. coli* DNA polymerase III. Cell *106*, 417–428.

Johnson, A., and O'Donnell, M. (2005). Cellular DNA replicases: components and dynamics at the replication fork. Annu. Rev. Biochem. *74*, 283–315.

Kelch, B.A., Makino, D.L., O'Donnell, M., and Kuriyan, J. (2011). How a DNA polymerase clamp loader opens a sliding clamp. Science *334*, 1675–1680.

Kelman, Z., and O'Donnell, M. (1995). DNA polymerase III holoenzyme: structure and function of a chromosomal replicating machine. Annu. Rev. Biochem. *64*, 171–200.

Kenakin, T. (1993). Radioligand binding experiments. In Pharmacologic Analysis of Drug-Receptor Interaction, Second Edition (San Diego: Raven Press), pp. 385–410.

Kohanski, M.A., Dwyer, D.J., and Collins, J.J. (2010). How antibiotics kill bacteria: from targets to networks. Nat. Rev. Microbiol. *8*, 423–435.

Kong, X.-P., Onrust, R., O'Donnell, M., and Kuriyan, J. (1992). Three-dimensional structure of the β subunit of *E. coli* DNA polymerase III holoenzyme: a sliding DNA clamp. Cell *69*, 425–437.

Kongsuwan, K., Josh, P., Picault, M.J., Wijffels, G., and Dalrymple, B. (2006). The plasmid RK2 replication initiator protein (TrfA) binds to the sliding clamp β subunit of DNA polymerase III: implication for the toxicity of a peptide derived from the amino-terminal portion of 33-kilodalton TrfA. J. Bacteriol. *188*, 5501–5509.

Krömker, V., Paduch, J.H., Abograra, I., Zinke, C., and Friedrich, J. (2011). [Effects of an additional nonsteroidal anti-inflammatory therapy with carprofen (Rimadyl Rind) in cases of severe mastitis of high yielding cows]. Berl. Munch. Tierarztl. Wochenschr. *124*, 161–167.

Leu, F.P., and O'Donnell, M. (2001). Interplay of clamp loader subunits in opening the β sliding clamp of *Escherichia coli* DNA polymerase III holoenzyme. J. Biol. Chem. *276*, 47185–47194.

Leu, F.P., Hingorani, M.M., Turner, J., and O'Donnell, M. (2000). The delta subunit of DNA polymerase III holoenzyme serves as a sliding clamp unloader in *Escherichia coli*. J. Biol. Chem. *275*, 34609–34618.

Lopez, S., Pertuy, S., Horspool, L., van Laar, P., and Rutten, A. (2007). Vedaprofen therapy in cats with upper respiratory tract infection or following ovariohysterectomy. J. Small Anim. Pract. *48*, 70–75.

López de Saro, F.J. (2009). Regulation of interactions with sliding clamps during DNA replication and repair. Curr. Genomics *10*, 206–215.

Mason, C.E., Jergic, S., Lo, A.T.Y., Wang, Y., Dixon, N.E., and Beck, J.L. (2013). *Escherichia coli* single-stranded DNA-binding protein: nanoESI-MS studies of salt-modulated subunit exchange and DNA binding transactions. J. Am. Soc. Mass Spectrom. *24*, 274–285.

Naktinis, V., Onrust, R., Fang, L., and O'Donnell, M. (1995). Assembly of a chromosomal replication machine: two DNA polymerases, a clamp loader, and sliding clamps in one holoenzyme particle. II. Intermediate complex between the clamp loader and its clamp. J. Biol. Chem. *270*, 13358–13365.

Oakley, A.J., Prosselkov, P., Wijffels, G., Beck, J.L., Wilce, M.C., and Dixon, N.E. (2003). Flexibility revealed by the 1.85 Å crystal structure of the β sliding-clamp subunit of *Escherichia coli* DNA polymerase III. Acta Crystallogr. D Biol. Crystallogr. *59*, 1192–1199.

Origlieri, C., and Bielory, L. (2009). Emerging drugs for conjunctivitis. Expert Opin. Emerg. Drugs *14*, 523–536.

Otwinowski, Z., and Minor, W. (1997). Processing of X-ray diffraction data collected in the oscillation mode. Methods Enzymol. *276*, 307–326.

Papadopoulos, J.S., and Agarwala, R. (2007). COBALT: constraint-based alignment tool for multiple protein sequences. Bioinformatics *23*, 1073–1079.

Pomerantz, R.T., and O'Donnell, M. (2007). Replisome mechanics: insights into a twin DNA polymerase machine. Trends Microbiol. *15*, 156–164.

Rigel, N.W., and Silhavy, T.J. (2012). Making a β-barrel: assembly of outer membrane proteins in Gram-negative bacteria. Curr. Opin. Microbiol. *15*, 189–193.

Robinson, A., Causer, R.J., and Dixon, N.E. (2012). Architecture and conservation of the bacterial DNA replication machinery, an underexploited drug target. Curr. Drug Targets *13*, 352–372.

Shamoo, Y., and Steitz, T.A. (1999). Building a replisome from interacting pieces: sliding clamp complexed to a peptide from DNA polymerase and a polymerase editing complex. Cell *99*, 155–166.

Shirin, H., Moss, S.F., Kancherla, S., Kancherla, K., Holt, P.R., Weinstein, I.B., and Sordillo, E.M. (2006). Non-steroidal anti-inflammatory drugs have bacteriostatic and bactericidal activity against *Helicobacter pylori*. J. Gastroenterol. Hepatol. *21*, 1388–1393.

Singh, N., Jabeen, T., Somvanshi, R.K., Sharma, S., Dey, S., and Singh, T.P. (2004). Phospholipase A2 as a target protein for nonsteroidal anti-inflammatory drugs (NSAIDS): crystal structure of the complex formed between phospholipase A2 and oxyphenbutazone at 1.6 Å resolution. Biochemistry *43*, 14577–14583.

Singh, N., Kumar, R.P., Kumar, S., Sharma, S., Mir, R., Kaur, P., Srinivasan, A., and Singh, T.P. (2009). Simultaneous inhibition of anti-coagulation and inflammation: crystal structure of phospholipase A2 complexed with indomethacin at 1.4 Å resolution reveals the presence of the new common ligand-binding site. J. Mol. Recognit. *22*, 437–445.

Skubák, P., Murshudov, G.N., and Pannu, N.S. (2004). Direct incorporation of experimental phase information in model refinement. Acta Crystallogr. D Biol. Crystallogr. *60*, 2196–2201.

Vonkeman, H.E., and van de Laar, M.A. (2010). Nonsteroidal anti-inflammatory drugs: adverse effects and their prevention. Semin. Arthritis Rheum. *39*, 294–312.

Wijffels, G., Dalrymple, B.P., Prosselkov, P., Kongsuwan, K., Epa, V.C., Lilley, P.E., Jergic, S., Buchardt, J., Brown, S.E., Alewood, P.F., et al. (2004). Inhibition of protein interactions with the β_2 sliding clamp of *Escherichia coli* DNA polymerase III by peptides from β_2-binding proteins. Biochemistry *43*, 5661–5671.

Wijffels, G., Johnson, W.M., Oakley, A.J., Turner, K., Epa, V.C., Briscoe, S.J., Polley, M., Liepa, A.J., Hofmann, A., Buchardt, J., et al. (2011). Binding inhibitors of the bacterial sliding clamp by design. J. Med. Chem. *54*, 4831–4838.

Winn, M.D., Ballard, C.C., Cowtan, K.D., Dodson, E.J., Emsley, P., Evans, P.R., Keegan, R.M., Krissinel, E.B., Leslie, A.G., McCoy, A., et al. (2011). Overview of the CCP4 suite and current developments. Acta Crystallogr. D Biol. Crystallogr. *67*, 235–242.

Wolff, P., Oliéric, V., Briand, J.P., Chaloin, O., Dejaegere, A., Dumas, P., Ennifar, E., Guichard, G., Wagner, J., and Burnouf, D.Y. (2011). Structure-based design of short peptide ligands binding onto the *E. coli* processivity ring. J. Med. Chem. *54*, 4627–4637.

Yin, Z., Kelso, M.J., Beck, J.L., and Oakley, A.J. (2013). Structural and thermodynamic dissection of linear motif recognition by the *E. coli* sliding clamp. J. Med. Chem. *56*, 8665–8673.

Zhou, H., Liu, W., Su, Y., Wei, Z., Liu, J., Kolluri, S.K., Wu, H., Cao, Y., Chen, J., Wu, Y., et al. (2010). NSAID sulindac and its analog bind RXRalpha and inhibit RXRalpha-dependent AKT signaling. Cancer Cell *17*, 560–573.